CHAPTER 14

ENHANCEMENT OF DIRECTIONAL WAVE SPECTRUM ESTIMATES[a]

by

Narayana N. Panicker,[1] M. ASCE

and

Leon E. Borgman[2]

ABSTRACT

Determination of the directional distribution of ocean surface waves is of practical importance and analytical schemes for it are developed and discussed here. Based on a generalized representation of wave properties such as surface elevation, subsurface pressure or horizontal components of water particle velocity, acceleration or wave force, two general schemes of analysis are developed. In one scheme the predictive equations for the directional distribution of both the amplitude and phase of waves are derived. Distribution of energy as a function of direction for random waves is obtained in the other scheme. Fourier series parameterization is used to represent directional spectrum. The truncation of the series dictated by data limitations introduce directional spread and negative side lobes for the estimated directional spectrum. A procedure to remove these undesirable side lobes by a non-negative smoothing function is described. The smoothing causes further directional spread. Methods for obtaining better directional resolution are discussed. Data adaptive spectral analysis techniques such as Maximum Likelihood Method and Maximum Entropy Method are suggested.

1. INTRODUCTION

The directional spectrum of ocean waves is a distribution of wave energy with both frequency and direction. This information is useful and necessary for understanding and predicting coastal processes like littoral sediment transport and diffraction and refraction of waves as well as for the prediction of motions and stresses in floating and fixed structures. Several different techniques of measurement and analysis are used for obtaining directional wave spectra. Panicker (17) gave a review of these techniques. A common method is the use of an array of wave gages to record wave properties at several different points in the wave field and analyze the data to obtain the directional spectral density distribution for each frequency of interest. Two analytical schemes were developed by the authors for the determination of directional spectra. The schemes are generalized by use of transfer functions between measured wave properties and surface wave amplitudes. These, an extension of the work reported in 1970 by Panicker and Borgman (14), are reported here. Fourier series parameterization is used to estimate directional spectrum but the limited number of gages in an array necessitates truncation of the Fourier series resulting in negative side lobes for the spectrum. A scheme for removing the negative side lobes by a non-negative smoothing function is developed and

---

[a]Contribution No. 3432 of Woods Hole Oceanographic Institution.

[1]Assistant Scientist, Ocean Engineering Department, Woods Hole Oceanographic Institution, Woods Hole, Massachusetts 02543, U.S.A.

[2]Professor of Geology and Statistics, University of Wyoming, Laramie, Wyoming 82070, U.S.A.

described. Truncated Fourier series and smoothing may reduce the directional resolution. Possible methods for obtaining higher directional resolution are also discussed.

2. ANALYTICAL SCHEMES

Two schemes of analysis are developed: the amplitude and phase detection scheme (Locked-Phase Analysis) and the spectrum approach (Random-Phase Analysis). A general representation of wave properties is used so that the resulting Fourier-Bessel expressions equally apply to array measurements of any wave property such as surface elevation, subsurface pressure, water particle velocity, water particle acceleration and linearized wave force.

2.1 General representation of a measurable wave parameter

The analytical schemes developed here are good for a general array in which the different sensors may be placed arbitrarily and measure not necessarily the same properties. Such a property, q, may be represented in terms of the wave amplitude, r, as

$$q = rh\left[U\cos(kx\cos\theta + ky\sin\theta - 2\pi ft + \phi) + V\sin(kx\cos\theta + ky\sin\theta - 2\pi ft + \phi)\right] . \tag{1}$$

Here the angular function, h, specifies the directional property of the measured parameter and

$$h = \begin{cases} 1, & \text{if the property measured is non-directional such as pressure} \\ \cos\theta, & \text{if the x-component of a property is measured} \\ \sin\theta, & \text{if the y-component is measured.} \end{cases}$$

(x,y,z) are the sensor coordinates with z measured positively downward from still-water level, k is the wave number (2π/wave length), θ the vector wave direction, and f the frequency, t is time elapsed and ϕ the corresponding phase angle. U(f,z) and V(f,z) are transfer functions for the various wave properties and are tabulated in Table 1. For facility for use in a general scheme of computation the wave properties in Table 1 are written in code in the first column of the table. The code is in the form of a 3-digit number of the form $w_1w_2w_3$ where w_1 is the property studied such as water level, pressure, etc., w_2 is information on relative water depth such as deep or shallow, and w_3 is the directionality information of the property. The following cases are studied:

w_1: 1 = water level, 2 = subsurface pressure, 3 = water particle velocity, 4 = water particle acceleration, 5 = force;

w_2: 0 = unaffected by depth, 1 = intermediate water depth, 2 = deep water;

w_3: 0 = non-directional property, 1 = x-component, 2 = y component.

The following additional notations are used in Table 1: ρ = water density, g = acceleration due to gravity, Z_2 = stillwater depth, C_D = coefficient of

Table 1. Transfer Functions for Wave Properties in Equation (1)

CODE $w_1 w_2 w_3$	U	V
100	1.0	0
210	$\rho g \frac{\cosh k(Z_2-z)}{\cosh kZ_2}$	0
220	$\rho g \exp(-kz)$	0
311	$2\pi f \frac{\cosh k(Z_2-z)}{\sinh kZ_2}$	0
312	0	$2\pi f \frac{\sinh k(Z_2-z)}{\sinh kZ_2}$
321	$2\pi f \exp(-kz)$	0
322	0	$2\pi f \exp(-kz)$
411	0	$(2\pi f)^2 \frac{\cosh k(Z_2-z)}{\sinh kZ_2}$
412	$-(2\pi f)^2 \frac{\sinh k(Z_2-z)}{\sinh kZ_2}$	0
421	0	$(2\pi f)^2 \exp(-kz)$
422	$-(2\pi f)^2 \exp(-kz)$	0
511	$C_D \frac{\rho}{2} D_P \sqrt{8/\pi}\, \sigma \frac{2\pi f \cosh k(Z_2-z)}{\sinh kZ_2}$	$C_M \rho \frac{\pi D_P^2}{4} (2\pi f)^2 \frac{\cosh k(Z_2-z)}{\sinh kZ_2}$
512	$-C_M \rho \frac{\pi D_P^2}{4} (2\pi f)^2 \frac{\sinh k(Z_2-z)}{\sinh kZ_2}$	$C_D \frac{\rho}{2} D_P \sqrt{8/\pi}\, \sigma \frac{2\pi f \sinh k(Z_2-z)}{\sinh kZ_2}$
521	$C_D \frac{\rho}{2} D_P \sqrt{8/\pi}\, \sigma\, 2\pi f \exp(-kz)$	$C_M \frac{\rho\pi D_P^2}{4} (2\pi f)^2 \exp(-kz)$
522	$-C_M \rho \frac{\pi D_P^2}{4} (2\pi f)^2 \exp(-kz)$	$C_D \frac{\rho}{2} D_P \sqrt{8/\pi}\, \sigma\, 2\pi f \exp(-kz)$

drag in force calculation, C_M = coefficient of mass in force calculation, D_p = diameter of object on which wave force is measured and σ = root-mean-square horizontal velocity of water particles in wave. Linear wave theory is used to obtain the quantities in Table 1 and in addition, linearization of drag force in the wave force expression is used for the transfer functions for force measurements (Borgman (4)).

2.2 Locked-Phase Analysis

2.2.2 General Development

Very often in the directional analysis of ocean waves the waves are assumed random and the computed directional spectrum does not retain any phase information. But for a phase-locked wave field as in some laboratory tanks or in some coastal regimes dominated by distant swells, an analysis procedure that would yield distribution of phase as well as amplitude as a function of wave direction may be appropriate. A deterministic scheme of analysis for it using the Fast Fourier Transform (FFT) technique is described below.

Let q_n be a wave parameter measured at time t_n on a sensor located at (x,y,z). Then q_n is the sum of the contributions from all the frequencies, $f_o \ldots f_M$, and directions θ_m. Let the component amplitudes for each frequency $m\Delta f$ be $r_m(\theta)$. Directions here are vector wave directions measured positive anti-clockwise from the X-axis. Using notations of Eq. 1 but substituting $\gamma = kx\cos\theta_m + ky\sin\theta_m$, one may write

$$q_n = \sum_{m=o}^{M} \int_{-\pi}^{\pi} r_m h\left[U\cos\{\gamma - 2\pi f_m t_n + \phi_m\} + V\sin\{\gamma - 2\pi f_m t_n + \phi_m\}\right] d\theta_m . \tag{2}$$

Let the duration of the record be T with a total of N data points. The FFT relationships involving data sampling interval Δt and frequency interval Δf are as follows:

$$\Delta t \cdot \Delta f = 1/N,\ \Delta f = 1/T,\ f_m = m\Delta f \quad \text{and} \quad t_n = n\Delta t. \tag{3}$$

Using these one can write down Eq. 2 as

$$q_n = \Delta f \sum_{m=o}^{M} B_m \cos\frac{2\pi mn}{N} + \Delta f \sum_{m=o}^{M} C_m \sin\frac{2\pi mn}{N} \tag{4}$$

where

$$B_m = T\int_{-\pi}^{\pi} r_m h\{U\cos(\gamma+\phi_m) + V\sin(\gamma+\phi_m)\}d\theta_m \tag{5}$$

and

$$C_m = T\int_{-\pi}^{\pi} r_m h\{U\sin(\gamma+\phi_m) - V\cos(\gamma+\phi_m)\}d\theta_m . \tag{6}$$

If we let $M = \frac{N}{2} - 1$ and let A_m as

$$A_m = \begin{cases} 0, & \text{if } m = M+1 = N/2 \\ \frac{1}{2}(B_m - i\,C_m), & \text{if } 1 \le m \le M = \frac{N}{2} + 1 \\ \frac{1}{2}(B_{N-m} + i\,C_{N-m}), & \text{if } \frac{N}{2} + 1 \le m \le N-1 \end{cases} \tag{7}$$

It can then be shown from Eqs. 4 and 7 that

$$q_n = \Delta f \sum_{m=o}^{N-1} A_m e^{i2\pi mn/N}. \tag{8}$$

A_m is thus the finite Fourier transform of q_n. They form a Fourier transform pair and A_m is given as

$$A_m = \Delta t \sum_{n=o}^{N-1} q_n e^{-i2\pi mn/N}. \tag{9}$$

$\bar{A}_m$, the complex conjugate of the FFT coefficient A_m of the time series at a gage for frequency $m\Delta f$, for $0 < m < N/2$, can now be written from Eqs. 5, 6, and 7 as

$$\bar{A}_m = \frac{T}{2}(U-iV) \int_{-\pi}^{\pi} r_m e^{i\phi_m} h\, e^{i(kx\cos\theta_m + ky\sin\theta_m)} d\theta_m \tag{10}$$

or

$$\frac{2\,\bar{A}_m}{T(U-iV)} = \int_{-\pi}^{\pi} r_m e^{i\phi_m} h\, e^{ikD\cos(\theta_m - \beta)} d\theta_m \tag{11}$$

where D is the radius vector from the origin to the gage, inclined at an angle β to the x-axis (see Fig. 1). The objective is to determine amplitude r_m and phase ϕ_m for each frequency $m\Delta f$ as a function of wave direction θ_m. Amplitude and phase may be either continuous or discrete functions of direction. Expressions for these two cases are derived below.

2.2.2 Continuous functions for amplitude and phase

Let the amplitude and phase function, $F(\theta)$, be expressed as a complex Fourier series:

$$F(\theta) = \frac{a_1 + ia'_o}{2} + \sum_{n=1}^{N} (a_n \cos n\theta + b_n \sin n\theta) + i \sum_{n=1}^{N} (a'_n \cos n\theta + b'_n \sin n\theta). \tag{12}$$

This can be written as an exponential Fourier series as

$$F(\theta) = \sum_{n=-N}^{N} \alpha_n e^{in\theta} \tag{13}$$

where

$$\alpha_n = \begin{cases} \frac{1}{2}\ (a_n + b'_n) + i(a'_n - b_n)\ , & \text{if } n > 0 \\ \frac{1}{2}\ (a_o + ia'_o), & \text{if } n = 0 \\ \frac{1}{2}\ (a_{-n} - b'_{-n}) + i(a'_{-n} + b_{-n})\ , & \text{if } n < 0 \end{cases} \tag{14}$$

Substituting Eq. 14 in Eq. 11 and dropping subscript m from θ, one gets

$$\frac{2\ \bar{\bar{A}}_m}{T(U-iV)} = \int_{-\pi}^{\pi} \sum_{n=-N}^{N} \alpha_n\ e^{in\theta} h\ e^{ikD\ \cos(\theta-\beta)} d\theta. \tag{15}$$

In the Locked-Phase analysis the function h is 1.0, $\cos\theta$ or $\sin\theta$ depending on the wave parameter measured being non-directional, x-component or y-component. In the Random-Phase analysis described in the next section, pairs of measurements are used and therefore, in general, instead of three there could be six angular functions $H(\theta)$ as defined in the exponential form below.

$$H = \sum_{r=-2}^{2} d_r\ e^{ir\theta} \tag{16}$$

where d_r is defined for the six different cases in Table 2 as follows:

Table 2. Values of d_r in Eq. 16

Case	$H(\theta)$	d_{-2}	d_{-1}	d_0	d_1	d_2
1	1.0 (h)	0	0	1	0	0
2	$\cos\theta$ (h)	0	$\frac{1}{2}$	0	$\frac{1}{2}$	0
3	$\sin\theta$ (h)	0	$\frac{1}{2}$	0	$-\frac{1}{2}$	0
4	$\cos^2\theta$	$\frac{1}{4}$	0	$\frac{1}{2}$	0	$\frac{1}{4}$
5	$\cos\theta\ \sin\theta$	$\frac{1}{4}$	0	0	0	$-\frac{1}{4}$
6	$\sin^2\theta$	$-\frac{1}{4}$	0	$\frac{1}{2}$	0	$-\frac{1}{4}$

Substituting Eq. 16 in Eq. 15 and $\psi = \theta - \beta$, one gets

$$\frac{2\ \bar{\bar{A}}_m}{T(U-iV)} = \sum_{n=-N}^{N} \alpha_n \sum_{r=-2}^{2} d_r \int_{-\pi}^{\pi} e^{i(n+r)(\psi+\beta)}\ e^{ikD\ \cos\psi} d\psi$$

$$= \sum_{n=-N}^{N} \alpha_n \sum_{r=-2}^{2} d_r\ e^{i(n+r)\beta} \left[\int_{-\pi}^{\pi} \cos(n+r)\psi\ e^{ikD\ \cos\psi} d\psi \right. \tag{17}$$

$$\left. + i \int_{-\pi}^{\pi} \sin(n+r)\psi\ e^{ikD\ \cos\psi} d\psi \right]$$

Abramowitz and Stegun (1) gives the value of the first integral as

$$\int_{-\pi}^{\pi} \cos(n+r)\psi \; e^{\imath kD \cos\psi} d\psi = 2\pi i^{n+r} J_{n+r}(kD) \tag{18}$$

where $J_{n+r}(kD)$ is the Bessel function of the first kind and order (n+r) with the argument kD. The value of the second integral is zero as the integrand is odd. Substituting this and α_n from Eq. 14 one gets

$$\frac{2\,\bar{A}_m}{T(U-\imath V)2\pi} = \frac{a_o + \imath a'_o}{2} \sum_{r=-2}^{2} d_r \, e^{\imath r\beta} \, \imath^r J_r(kD)$$

$$+ \sum_{n=1}^{N} \frac{1}{2}\left[(a_n + b'_n) + \imath(a'_n - b_n)\right] \sum_{r=-2}^{2} d_r \, e^{\imath(n+r)\beta} \, \imath^{n+r} J_{n+r}(kD) \tag{19}$$

$$+ \sum_{n=1}^{N} \frac{1}{2}\left[(a_n - b'_n) + \imath(a'_n + b_n)\right] \sum_{r=-2}^{2} d_r e^{-\imath(n-r)\beta} \, \imath^{-n+r} J_{-n+r}(kD)$$

Equation 19 can be simplified by noting that

$$J_{-r}(kD = (-1)^r J_r(kD) \text{ and } \imath^{-r} J_{-r}(kD) = i^r J_r(kD)$$

and assigning for various cases in Table 2 a dummy parameter ε as follows:

$$\varepsilon = \begin{cases} 1.0, \text{ for cases } 1, 4, 5, 6 \\ \imath \;, \text{ for cases } 2, 3 \end{cases}$$

Let

$$A^*_o = \frac{d_o J_o(kD)}{\varepsilon} + \sum_{r=1}^{2} \frac{d_r \, e^{\imath r\beta} + d_{-r} e^{-\imath r\beta}}{\varepsilon} \imath^r \, J_{n+r}(kD) \tag{20}$$

$$A^*_n = \sum_{r=-2}^{2} \frac{d_r \, e^{\imath(n+r)\beta} + d_{-r} \, e^{-i(n+r)\beta}}{\varepsilon} \imath^r \, J_{n+r}(kD) \tag{21}$$

$$B^*_n = \sum_{r=-2}^{2} \frac{-\imath d_r \, e^{i(n+r)\beta} + \imath d_{-r} \, e^{-i(n+r)\beta}}{\varepsilon} \imath^r \, J_{n+r}(kD) \tag{22}$$

Then Eq. 19 can be expressed as

$$\frac{2\,\bar{A}_m}{T(U-\imath V)\pi\varepsilon} = (a_o + \imath a'_o)A^*_o + \sum_{n=1}^{N} \imath^n (a_n A^*_n + b_n B^*_n)$$

$$+ \sum_{n=1}^{N} i^{n+1} \, (a'_n A^*_n + b'_n B^*_n). \tag{23}$$

It may be noted that A_o^*, A_n^*, and B_n^* are all real-valued functions. They are evaluated and tabulated in Table 3. Equation 23 is the desired relationship for evaluating the directional function $F(\theta)$ for frequency $m\Delta f$ in terms of its Fourier series coefficients a_o, a_o', a_1, a_1', etc. and expressions similar to it exist for other frequencies. Equation 23 may be written in matrix form as follows:

$$Re\ \frac{2\,\overline{A}_m}{T(U-iV)\pi} = \left[A_o^*,\ -A_1^*,\ -B_1^*,\ -A_2^*,\ -B_2^*,\ldots\right]\left[a_o,\ a_1',\ b_1',\ a_2,\ b_2,\ldots\right]^T \tag{24}$$

$$Im\ \frac{2\,\overline{A}_m}{T(U-iV)\pi} = \left[A_o^*,\ A_1^*,\ B_1^*,\ -A_2^*,\ -B_2^*,\ldots\right]\left[a_o',\ a_1,\ b_1,\ a_2',\ b_2',\ldots\right]^T \tag{25}$$

Here superscript T denotes a transpose of the matrix indicated. By inverting the matrices the coefficients for the complex Fourier series can be obtained and the directional distribution functions for amplitude a_m and phase ϕ_m for each frequency $m\Delta f$ can be evaluated as follows:

$$r_m(\theta) = \left[\left\{\frac{a_o}{2} + \sum_{n=1}^{N}(a_n\cos n\theta + b_n \sin n\theta)\right\}^2 + \left\{\frac{a_o'}{2} + \sum_{n=1}^{N}(a_n' \cos n\theta + b_n' \sin n\theta)\right\}^2\right]^{1/2} \tag{26}$$

$$\phi_m(\theta) = \arctan\left\{\frac{\frac{a_o'}{2} + \sum_{n=1}^{N}(a_n' \cos n\theta + b_n' \sin n\theta)}{\frac{a_o}{2} \sum_{n=1}^{N}(a_n \cos n\theta + b_n \sin n\theta)}\right\} \tag{27}$$

2.2.3 Amplitudes and Phases of Discrete Wave Trains

In the discrete case the complex phase-amplitude function $F(\theta)$ is assumed to have non-zero values only at a finite number of discrete directions. $F(\theta)$ may be written as

$$F(\theta) = \sum_{m=1}^{M}(r_m + ir_m')\delta(\theta-\theta_m) \tag{28}$$

where $\delta(\theta-\theta_m)$ is a Dirac delta function representing a spike at $\theta = \theta_m$ and zero elsewhere. A relationship analogous to Eq. 11 can be used to evaluate $F(\theta)$.

Table 3. Values of A_o^*, A_n^*, and B_n^* for Different Cases

(All Bessel functions, J_n, here have argument kD)

Case	$H(\theta)$	ε	A_o^*	A_n^*	B_n^*
1	1.0	1.0	J_o	$2 J_n \cos n\beta$	$2 J_n \sin n\beta$
2	$\cos\theta$	i	$J_1 \cos\beta$	$-J_{n-1} \cos(n-1)\beta$ $+J_{n+1} \cos(n+1)\beta$	$-J_{n-1} \sin(n-1)\beta$ $+J_{n+1} \sin(n+1)\beta$
3	$\sin\theta$	1	$J_1 \sin\beta$	$J_{n-1} \sin(n-1)\beta$ $+J_{n+1} \sin(n+1)\beta$	$-J_{n-1} \cos(n-1)\beta$ $-J_{n+1} \cos(n+1)\beta$
4	$\cos^2\theta$	1.0	$\frac{1}{2}(J_o - J_2 \cos^2\beta)$	$J_n \cos n\beta - \frac{1}{2} J_{n-2} \cos(n-2)\beta$ $- \frac{1}{2} J_{n+2} \cos(n+2)\beta$	$J_n \sin n\beta - \frac{1}{2} J_{n-2} \sin(n-2)\beta$ $- \frac{1}{2} J_{n+2} \sin(n+2)\beta$
5	$\cos\theta \sin\theta$	1.0	$-\frac{1}{2}(J_2 \sin^2\beta)$	$\frac{1}{2} J_{n-2} \sin(n-2)\beta$ $- \frac{1}{2} J_{n+2} \sin(n+2)\beta$	$-\frac{1}{2} J_{n-2} \cos(n-2)\beta$ $+ \frac{1}{2} J_{n+2} \cos(n+2)\beta$
6	$\sin^2\theta$	1.0	$\frac{1}{2}(J_o + J_2 \cos^2\beta)$	$J_n \cos n\beta + \frac{1}{2} J_{n-2} \cos(n-2)\beta$ $+ \frac{1}{2} J_{n+2} \cos(n+2)\beta$	$J_n \sin n\beta + \frac{1}{2} J_{n-2} \sin(n-2)\beta$ $+ \frac{1}{2} J_{n+2} \sin(n+2)\beta$

$$\frac{2\,\bar{A}_m}{T(U-iV)} = \int_{-\pi}^{\pi} Fh\, e^{ikD\cos(\theta_m-\beta)}\, d\theta \tag{29}$$

Substituting for F from Eq. 28 and for h with appropriate values of $H(\theta_m)$ from Table 2 and evaluating the integral involving Dirac delta function, one gets

$$\frac{2\,\bar{A}_m}{T(U-iV)} = \sum_{m=1}^{M} (r_m + r'_m)H(\theta_m)e^{ikD\cos(\theta_m-\beta)} \tag{30}$$

Separating the real and imaginary parts of Eq. 30 one can obtain as many pairs of equations as there are gages, for r_m and r'_m.

$$Re\,\frac{2\,\bar{A}_m}{T(U-iV)} = \sum_{m=1}^{M}\left[r_m H(\theta_m)\cos kD\cos(\theta_m-\beta)\right] - \sum_{m=1}^{M}\left[r'_m H(\theta_m)\sin kD\cos(\theta_m-\beta)\right] \tag{31}$$

$$Im\,\frac{2\,\bar{A}_m}{T(U-iV)} = \sum_{m=1}^{M}\left[r_m H(\theta_m)\sin kD\cos(\theta_m-\beta)\right] + \sum_{m=1}^{M}\left[r'_m H(\theta_m)\cos kD\cos(\theta_m-\beta)\right] \tag{32}$$

A least-square analysis is appropriate for obtaining r_m and r'_m from Eq. 31 and Eq. 32. By computing the modulus and argument from r_m and r'_m one obtains the wave amplitude and phase respectively.

2.3 Random-Phase Analysis

2.3.1 General Development

Randomness in an ocean wave field may be introduced by assuming phase angles to be random variables. Let the phase angle be an independent random variable uniformly distributed over the interval $-\pi$ to π. Let the directional spectral density function $S(f,\theta)$ for $f > 0$ and $-\pi \leq \theta < \pi$ be such that the total energy E contained in the waves traveling in the direction between $\theta - \frac{\Delta\theta}{2}$ and $\theta + \frac{\Delta\theta}{2}$ and having frequencies between $f - \frac{\Delta f}{2}$ and $f + \frac{\Delta f}{2}$ is

$$E = \int_{\theta-\frac{\Delta\theta}{2}}^{\theta+\frac{\Delta\theta}{2}} \int_{f-\frac{\Delta f}{2}}^{f+\frac{\Delta f}{2}} 2\rho g S(f,\theta)\,df\,d\theta \tag{33}$$

where ρ is water density and g the acceleration of gravity. However, the total energy per unit crest width and unit wavelength of a wavelet of amplitude, r is $\rho g r^2/2$. When Δf and $\Delta\theta$ are sufficiently small one can therefore write an equivalent surface wave amplitude in terms of the directional spectral density

$$r \simeq \sqrt{4S(f,\theta)\Delta f\ \Delta\theta} \tag{34}$$

After Pierson and Marks (18) one may therefore represent the random sea surface as the following pseudo-integral

$$q(x,y,t) = 2\int_0^{\infty}\int_{-\pi}^{\pi}\sqrt{S(f,\theta)df\ d\theta}\cos(kx\cos\theta + ky\sin\theta - 2\pi ft + \phi) \tag{35}$$

The above pseudo-integral should be considered only as a concise and descriptive symbolization of the limiting process indicated and not as an actual integral. $q(x,y,t)$ is a Gaussian stochastic process in the three parameters x, y, and t; see Takano (19, p. 86).

Let q' be any wave parameter at time t and measured at a gage located at (x,y,z') and let q" be a wave parameter measured at time t + τ and another gage located at (x+X, y+Y, z"). Analogous to Eq. 2 with corresponding primes for circular functions h and transfer functions U and V, and using Eq. 35, one may write down q' and q" as follows

$$q' = 2\int_0^{\infty}\int_0^{2\pi}\sqrt{S\ df\ d\theta}\ h'\left[U'\cos\{kx\cos\theta + ky\sin\theta - 2\pi ft + \phi\}\right. \\ \left. + V'\sin\{kx\cos\theta + ky\sin\theta - 2\pi ft + \phi\}\right] \tag{36}$$

$$q'' = 2\int_0^{\infty}\int_0^{2\pi}\sqrt{S\ df\ d\theta}\ h''\left[U''\cos\{k(x+X)\cos\theta + k(y+Y)\sin\theta - 2\pi f(t+\tau) + \phi\}\right. \\ \left. + V''\sin\{k(x+X)\cos\theta + k(y+Y)\sin\theta - 2\pi f(t+\tau) + \phi\}\right] \tag{37}$$

The cross-covariance $C_{q'q''}$ between q' and q" is the expectation of the product q'q". Evaluating the expectations of the various terms in the product and substituting $\gamma = kX\cos\theta + kY\sin\theta$, the cross-covariance between measurements at the two gages can be written in terms of the co-spectrum c(f) and quadrature spectrum q(f) as follows.

$$C_{q'q''} = 2\int_0^{\infty} c(f)\cos 2\pi f\tau df + 2\int_0^{\infty} q(f)\sin 2\pi f\tau df \tag{38}$$

where

$$c(f) = \int_0^{2\pi} Sh'h''\left[(U'U'' + V'V'')\cos\gamma + (U'V'' - V'U'')\sin\gamma\right]d\theta \tag{39}$$

$$q(f) = \int_0^{2\pi} Sh'h''\left[(U'U'' + V'V'')\sin\gamma - (U'V'' - V'U'')\cos\gamma\right]d\theta\ . \tag{40}$$

The cross-spectrum is defined as c - iq. It may be obtained as the product the complex conjugate of FFT coefficient of one gage record with the FFT

coefficient of the other and divided by the duration of the record. The complex conjugate of the cross-spectrum may be written as

$$c + iq = \left[(U'U'' + V'V'') + i(V'U'' - U'V'')\right] \int_0^{2\pi} Sh'h''e^{i\gamma}d\theta \ . \qquad (41)$$

If we let D and β be the spacing and orientation between two gages of a pair (see Fig. 1) and $h'h'' = H(\theta)$ be one of the circular functions noted in Table 2, Eq. 41 can be written as

$$\frac{c + iq}{(U'+iV')(U''-iV'')} = \int_0^{2\pi} SH\, e^{ikD\cos(\theta-\beta)}d\theta. \qquad (42)$$

This expression can be used to evaluate the directional spectral density function $S(f,\theta)$. Two cases may be considered $S(\theta)$ for each frequency as a continuous function of direction and $S(\theta)$ discrete in directions.

2.3.2 Continuous Function for Directional Spectrum

When wave energy is distributed continuously around the circle, $S(\theta)$ may be represented as a Fourier series.

$$S(\theta) = \frac{a_o}{2} + \sum_{n=1}^{N} (a_n \cos n\theta + b_n \sin n\theta). \qquad (43)$$

This is equivalent to the series obtained by setting the imaginary part zero in the complex Fourier series representation in Eq. 12 of the Locked-Phase Analysis. The results derived there may be used here with suitable modification and the following equations analogous to Eq. 24 and Eq. 25 are obtained.

$$Re\ \frac{c + iq}{(U'+iV')(U''-iV'')\pi\varepsilon} = \left[A_o^*, -A_2^*, -B_2^*, A_4^*, B_4^*, \ldots\right]\left[a_o, a_2, b_2, a_4, b_4, \ldots\right]^T \qquad (44)$$

$$Im\ \frac{c + iq}{(U'+iV')(U''-iV'')\pi\varepsilon} = \left[A_1^*, B_1^*, -A_3^*, -B_3^*, \ldots\right]\left[a_1, b_1, a_3, b_3, \ldots\right]^T \ . \qquad (45)$$

Here A_o^*, A_1^*, B_1^*, etc. are as tabulated in Table 3. The Fourier series coefficients a_o, a_1, b_1, etc. of the directional spectral density function $s(\theta)$ may be obtained by matrix inversion. As there are as many cross-spectra between gages as there are pairs of gages, the number of equations available is equal to the number of pairs of gages. That is, the greatest number of harmonics up to which $S(\theta)$ can be represented is at the most the number of gage pairs.

2.3.3 Discrete Energy Analysis

If $S(\theta)$ has non-zero values only at a finite number of directions, an analysis analogous to the one in Section 2.2.3 may be made by representing

$S(\theta)$ in terms of a Dirac delta function.

$$S(\theta) = \sum_{m=1}^{M} r_m \, \delta(\theta-\theta_m) \tag{46}$$

The following results similar to Eq. 31 and Eq. 32 may be obtained.

$$Re \frac{c + iq}{(U'+iV')(U''-iV'')} = \sum_{m=1}^{M} r_m \, H(\theta_m) \cos kD \cos(\theta_m-\beta) \tag{47}$$

$$Im \frac{c + iq}{(U'+iV')(U''-iV'')} = \sum_{m=1}^{M} r_m \, H(\theta_m) \sin kD \cos(\theta_m-\beta) \tag{48}$$

The discrete energy values r_m for each direction θ_m may be obtained from Eq. 47 and Eq. 48 by a least-square analysis.

3. SMOOTHING OF DIRECTIONAL SPECTRUM

When a Fourier series parameterization is used to represent directional spectrum as in Eq. 43, the quality of the result will depend greatly with the total number of harmonics of the Fourier series representation. The number of Fourier series coefficients that can be evaluated from the data, however, is limited by the number of gages and their placement in an array. The maximum number of harmonics that can be evaluated by the Random-Phase Analysis is at the most equal to the number of pairs of gages in an array and half the number of gages by the Locked-Phase Analysis. All but the first terms of a Fourier series take negative values and therefore negative side lobes show up when directional spectrum is represented by a truncated Fourier series. The negative side lobes in an energy spectrum is objectionable because energy spectral density is non-negative. It is undesirable also because negative side lobes may mask the real signals at the corresponding directions and therefore deteriorate directional resolution. Longuet-Higgins (11) proposed methods to use the available Fourier coefficients to fit the data best to a limited number of principal directions by making use of the fact that the real spectrum is non-negative. But when the directional spectrum is a unimodal continuous distribution for each frequency its estimation may be enhanced by convoluting it with a non-negative smoothing function to remove the negative side lobes. Smoothing functions for directional spectra were proposed and used by Longuet-Higgins, Cartwright and Smith (12). A procedure for using one such smoothing function $W_2(\theta)$, suggested by Borgman (5) is described below.

$$W_2(\theta) = R_N \cos^{2N}(\theta/2) \tag{49}$$

where N is the total number of harmonics. R_N is such that the area under $W_2(\theta)$ is unity and the value of the effective width (width of a rectangle of the same height and equal area) is the reciprocal of R_N. Let the unsmoothed directional

spectrum be represented as a Fourier series:

$$S(\theta) = \frac{a_o}{2} + \sum_{k=1}^{N} (a_k \cos k\theta + b_k \sin k\theta) \tag{50}$$

Let $W_2(\theta)$ be expressed as a Fourier series as follows:

$$W_2(\theta) = \frac{1}{2\pi} + \frac{1}{\pi} \sum_{k=1}^{N} C_{kN} \cos(k\theta) \tag{51}$$

where C_{kN} have to be evaluated consistent with Eq. 49. Convoluting $S(\theta)$ with $W_2(\theta)$ of Eq. 51, one gets the smoothed spectrum $S_2(\theta)$ as follows:

$$\begin{aligned} S_2(\theta) &= \int_{-\pi}^{\pi} S(\theta')W_2(\theta-\theta')d\theta' \\ &= \frac{a_o}{2} + \sum_{k=1}^{N} C_{kN}(a_k \cos k\theta + b_k \sin k\theta) \end{aligned} \tag{52}$$

Thus to obtain the smoothed spectrum one only has to evaluate the coefficients C_{kN}. This can be done by expanding Eq. 49 in the form of the Fourier series in Eq. 51. Details of a numerical procedure for this is given by Panicker (16). The coefficients are computed for each of the Fourier series representations up to the one with a maximum of 8 harmonics and tabulated in Table 4.

4. DIRECTIONAL RESOLUTION

The analytical procedures developed in the previous sections were applied to actual data to obtain directional spectra. The necessary computer programs were developed and described along with the details of the analysis by Panicker (16). Some results obtained are shown here in the context of a discussion on directional resolution.

Smoothing of the directional spectrum causes a broadening of the directional spread. This can be seen in Fig. 2 where the results obtained for a simulated single sinusoid with a 4-gage star array are shown. One notices that the effective width of the directional spectrum represented to 4 harmonics and obtained with W_2 smoothing is about 98^o and without smoothing the effective width is 40^o, but the ideal result for the single sinuoid would be a single spike at the input direction with no directional spread. This indicates an inherent directional spread on account of the truncated Fourier series representation of directional spectrum and an additional spread owing to W_2 smoothing which is necessary to remove the negative side lobes of the truncated series. However, when real data from the ocean is used to obtain directional spectrum, as done by Panicker and Borgman (14), it is not obvious how much of the directional spread is real and how much is due to the truncation and smoothing of the Fourier series. Figures 3 and 4 are directional

Table 4. values of R_N and C_{kN} for $W_2(\theta)$

No. of Harmonics N	Reciprocal of Effective Width R_N	Fourier Coefficients, C_{kN}							
		k=1	2	3	4	5	6	7	8
1	$\frac{1}{\pi}$	$\frac{1}{2}$							
2	$\frac{4}{3\pi}$	$\frac{2}{3}$	$\frac{1}{6}$						
3	$\frac{8}{5\pi}$	$\frac{3}{4}$	$\frac{3}{10}$	$\frac{1}{20}$					
4	$\frac{64}{35\pi}$	$\frac{4}{5}$	$\frac{2}{5}$	$\frac{4}{35}$	$\frac{1}{70}$				
5	$\frac{128}{63\pi}$	$\frac{5}{6}$	$\frac{10}{21}$	$\frac{5}{28}$	$\frac{5}{126}$	$\frac{1}{252}$			
6	$\frac{512}{231\pi}$	$\frac{6}{7}$	$\frac{15}{28}$	$\frac{5}{21}$	$\frac{1}{14}$	$\frac{1}{77}$	$\frac{1}{924}$		
7	$\frac{1024}{429\pi}$	$\frac{7}{8}$	$\frac{7}{12}$	$\frac{7}{24}$	$\frac{7}{66}$	$\frac{7}{264}$	$\frac{7}{1716}$	$\frac{7}{3432}$	
8	$\frac{16384}{6435\pi}$	$\frac{8}{9}$	$\frac{28}{45}$	$\frac{56}{165}$	$\frac{14}{99}$	$\frac{56}{1287}$	$\frac{4}{429}$	$\frac{8}{6435}$	$\frac{1}{12870}$

spectra obtained for two different frequencies from the CERC 5-gage array designed by Borgman and Panicker (6) and installed off Pt. Mugu, California by the U. S. Army Corps of Engineers. It may be seen that W_2 smoothing removes the spurious side lobes resulting from the truncation of Fourier series. One, however, suspects that W_2 smoothing has caused broadening of the directional band width and reduction of directional resolution.

It might be emphasized that higher directional resolution does not necessarily associate itself with a narrow directional spectrum. The highest directional resolution ($\pm 3^{o}$) achieved so far for ocean wave measurements is for the directional spectra of 7 sec waves obtained by a radio back-scatter technique off Wake Island, Pacific Ocean and reported by Teague, et al. (20). The most interesting feature of these high-resolution directional spectra is their broad directional band width with as much as 1% of the peak energy density showing up at directions opposite to the wind. Longuet-Higgins, Cartwright and Smith (12) also reported broad directional spectra, but the results obtained by them using a pitch-roll buoy and Fourier series parameterization with smoothing were not considered to have sufficient resolution to support the conclusion. However, the results of Teague, et al. (20) warn against restrictive assumptions on directional spread about the mean wind direction, such as $\pm 45^{o}$ of

Arthur (2) and $\pm 90^{\circ}$ of Cote, et al. (9). Arbitrary parameterizations such as the tent functions of Oakley (13) to fit the data to narrow directional spectra also may not be the appropriate methods for ocean waves.

As Teague, et al. (20) has shown, high resolution directional spectra can be obtained by good measurement techniques. On the analysis side, data adaptive techniques of analysis [Lacoss (10)] for array data hold promise for high resolution. Maximum Likelihood Method [Capon (8)] and Maximum Entropy Method [Burg (7)] are two such nonlinear techniques. A review of these are given by Panicker (17). The advantage of these methods is that arbitrary parameterizations such as Fourier series representation are not used but the data content is used to determine the window shape. The analytical development described in Section 2.31 of this paper would be applicable for the Maximum Likelihood Method also. O. H. Oakley (personal communication) computed directional spectra using the Maximum Likelihood Method and obtained good directional resolution with a 4-gage star array. In this method only an additional Hermitian matrix inversion is required and therefore the computer time requirements are comparable to those for the direct Fourier transform method of Barber (3). Lacoss (10) and Burg (7) reported that Maximum Entropy Method gave still higher resolution; but Burg (7) noted that with arrays having unequal spacings the determination of the Maximum Entropy Spectrum became very difficult. This is still subject to active research.

5. SUMMARY AND CONCLUSIONS

Two general schemes for the directional analysis of surface waves have been developed and described. A generalized representation of wave properties was used so that the equations derived are applicable to the analysis of different kinds of measurements such as surface elevation, subsurface pressure or either of the horizontal components of water particle velocity, acceleration or wave force. The necessary transfer functions were tabulated. The amplitude and phase detection scheme (Locked-Phase Analysis) is a deterministic, Fast Fourier Transform method to determine the distribution of amplitude and phase as a function of direction and is applicable to phase-locked systems such as wave fields in some laboratory tanks and some coastal regimes dominated by distant swells. Cases of amplitudes and phases both as continuous functions of directions and discrete were considered. The Random-Phase Analysis is a spectrum approach to obtain the distribution of wave energy density as a function of direction for each frequency and both continuous and discrete distributions were considered. Fourier series parameterization was used for the directional distribution functions and explicit equations were derived for calculating the Fourier series coefficients. There are two such equations for each gage in the Locked-Phase Analysis and for each gage-pair in the Random-Phase Analysis. The evaluation of the Fourier series coefficients is done by inverting a matrix of quantities describing the array geometry relative to wave length and multiplying it with a matrix of quantities derived from the FFT coefficients of sensor outputs as stated in Eq. (24) and Eq. (25) for Locked-Phase Analysis and Eq. (44) and Eq. (45) for Random Phase Analysis. It was noted that representation of directional spectrum by truncated Fourier series resulted in negative side lobes for the spectrum. Negative side lobes for spectrum are unrealistic and undesirable and they have to be removed. Computational procedure for this by use of the non-negative W_2 smoothing function was described.

Results obtained using data from simulation and from the CERC 5-gage array off Point Mugu, California were discussed. It was found that representation by a truncated Fourier series introduced considerable directional spread to a simulated sinusoid and W_2 smoothing caused further directional spread. Better directional resolution than that obtained by Fourier series parameterization would be desirable.

High directional resolution does not necessarily go with narrow directional spectrum. A directional sprectrum obtained by radio backscatter technique was found to have the highest directional resolution so far reported, yet the spectrum itself was broad showing considerable energy values in all directions. Therefore arbitrary parameterizations such as tent functions for narrow spectra may not yield high directional resolution for ocean waves.

For analysis to obtain high resolution directional spectra from wave gage arrays, data adaptive techniques of analysis such as Maximum Likelihood Method and Maximum Entropy Method hold promise. The general scheme of analysis reported here may also be used for a Maximum Likelihood estimation in lieu of the Fourier series parameterization described.

ACKNOWLEDGMENT

The prepartion of this paper was partially supported by U. S. Navy ONR Contract N00014-74-C-0262 at the Woods Hole Oceanographic Institution. The work reported here was mostly conducted at the University of California, Berkeley with partial support from the Coastal Engineering Research Center of U. S. Army Corps of Engineers through contract DACW72-68-C-0016. The advice and support of Professor R. L. Wiegel are greatly appreciated.

APPENDIX 1. REFERENCES

1. Abramowitz, M. and Stegun, I. A., "Handbook of Mathematical Functions," Dover Publications, New York, 1965.

2. Arthur, R. S., "Variability in Direction of Wave Travel," Ocean Surface Waves, Annals of New York Academy of Science, Vol. 51, pp. 511-521, 1949.

3. Barber, N. F., "The Direçtional Resolving Power of an Array of Wave Detectors," Ocean Wave Spectra, Prentice-Hall, Inc., Englewood Cliffs, N. J., pp. 137-150, 1961.

4. Borgman, L. E., "Ocean Wave Simulation for Engineering Design," Proceedings, ASCE Conference on Civil Engineering in the Oceans, San Francisco, pp. 31-74, September 1967.

5. Borgman, L. E., "Directional Spectra Models for Design Use for Surface Waves," Technical Report HEL 1-12, Hydraulic Engineering Laboratory, University of California, Berkeley, June 1969.

6. Borgman, L. E. and N. N. Panicker, "Design Study for a Suggested Wave Gage Array off Point Mugu, California," Technical Report HEL 1-14, Hydraulic Engineering Laboratory, University of California, Berkeley, January 1970.

7. Burg, J. P., "The Relationship Between Maximum Entropy Spectra and Maximum Likelihood Spectra," Geophysics, Vol. 37, No. 2, pp. 375-376, April 1972.

8. Capon, J., "High-Resolution Frequency-Wave Number Spectrum Analysis," Proceedings of the IEEE, Vol. 57, No. 8, pp. 1408-1418, August 1969.

9. Cote, L. J., J. O. Davis, W. Marks, R. J. McGough, E. Mehr, W. J. Pierson, J. F. Ropek, G. Stephenson, and R. C. Vetter, "The Directional Spectrum of a Wind Generated Sea as Determined from Data Obtained by the Stereo Wave Observation Project," Meteorological Papers, Vol. 2, No. 6, New York University, June 1960.

10. Lacoss, R. T., "Data Adaptive Spectral Analysis Methods," Geophysics, Vol. 36, No. 4, pp. 661-675, August 1971.

11. Longuet-Higgins, M. S., "Bounds for the Integral of a Non-negative Function in Terms of its Fourier Coefficients," Proceedings, Cambridge Philosophical Society, Vol. 51, part 4, pp. 590-603, October 1955.

12. Longuet-Higgins, M. S., D. E. Cartwright, and N. D. Smith, "Observations of the Directional Spectrum of Sea Waves Using the Motions of a Floating Buoy," Ocean Wave Spectra, Prentice-Hall, Inc., Englewood Cliffs, N. J., pp. 111-136, 1963.

13. Oakley, O. H., "Directional Wave Spectra Measurement and Analysis Systems," presented at the SNAME Seakeeping Symposium, '20th Anniversary of St. Denis-Pierson paper,' Webb Institute of Naval Architecture, October 1973.

14. Panicker, N. N. and L. E. Borgman, "Directional Spectra from Wave Gage Arrays," Proceedings, 12th International Conference on Coastal Engineering, Washington, D. C., pp. 117-136, September 13-18, 1970.

15. Panicker, N. N. and L. E. Borgman, "Computer Simulation for the Design of Wave-Gage Arrays," Proceedings, 1971 Summer Computer Simulation Conference, Boston, Massachusetts, pp. 861-867, July 1971.

16. Panicker, N. N., "Determination of Directional Spectra of Ocean Waves from Gage Arrays," Technical Report HEL 1-18, University of California, Berkeley, p. 315, August 1971.

17. Panicker, N. N. "Review of Techniques for Directional Wave spectra," Proceedings, International Symposium on Ocean Wave Measurement and Analysis (WAVES 74), New Orleans, September 1974.

18. Pierson, W. J. and W. Marks., "The Power Spectrum Analysis of Ocean Wave Records," Transactions, American Geophysical Union, Vol. 33, 1952.

19. Takano, K., "On Some Limit Theorems of Probability-Distributions," Annals of the Institute of Statistical Mathematics, Tokyo, Vol. 6, pp. 37-113, 1954.

20. Teague, C. C., G. L. Tyler, J. W. Joy, and R. H. Stewart, "Synthetic Aperture Observations of Directional Height Spectra for 7s Ocean Waves," Nature Physical Science, Vol. 244, No. 137, pp. 98-100, August 13, 1973.

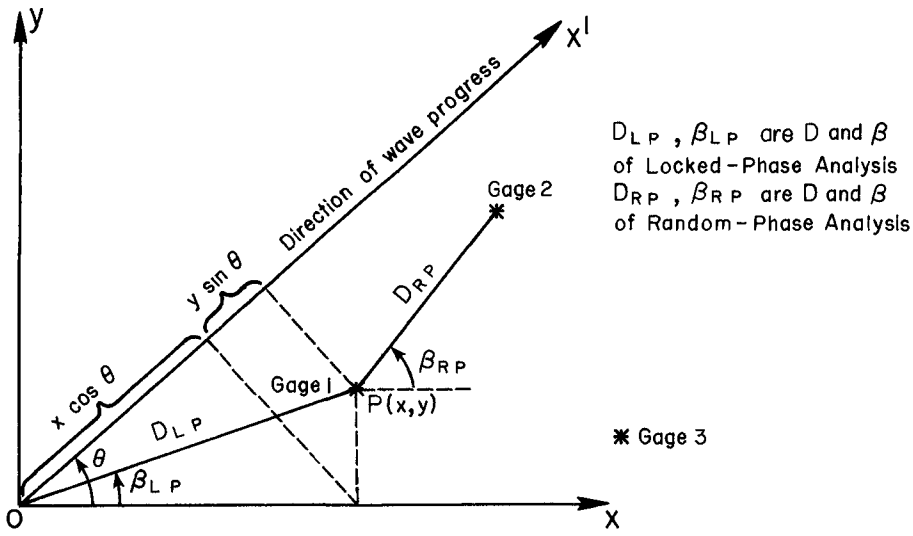

FIG. 1 DEFINITION SKETCH FOR WAVE DIRECTION ANALYSIS

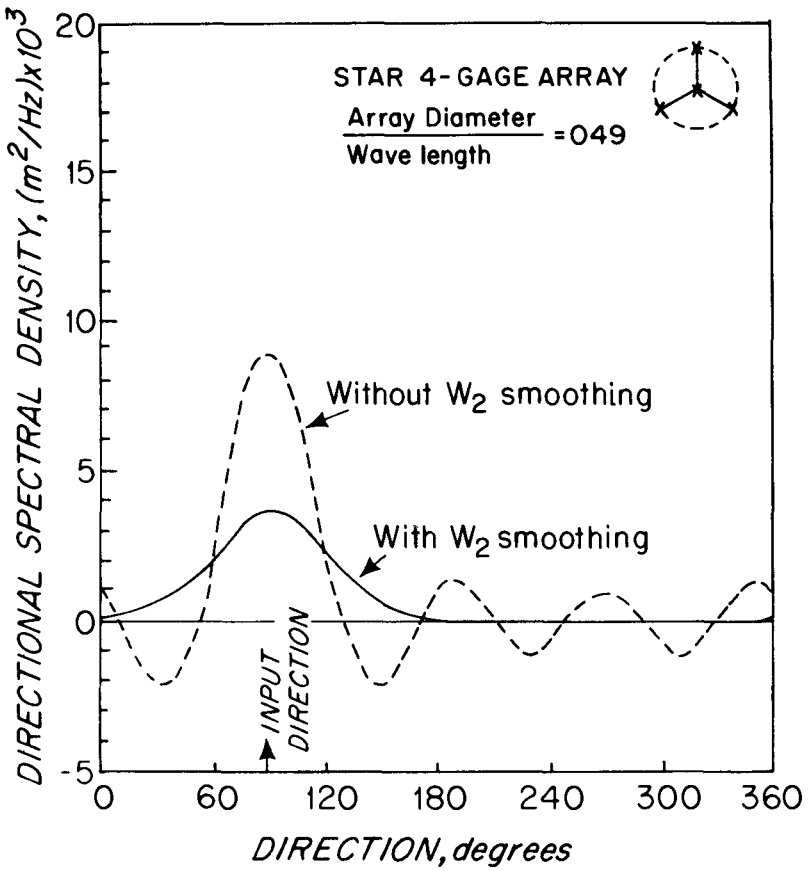

FIG. 2. FOURIER SERIES REPRESENTATION OF DIRECTION OF A SINGLE WAVE TRAIN USING FOUR HARMONICS

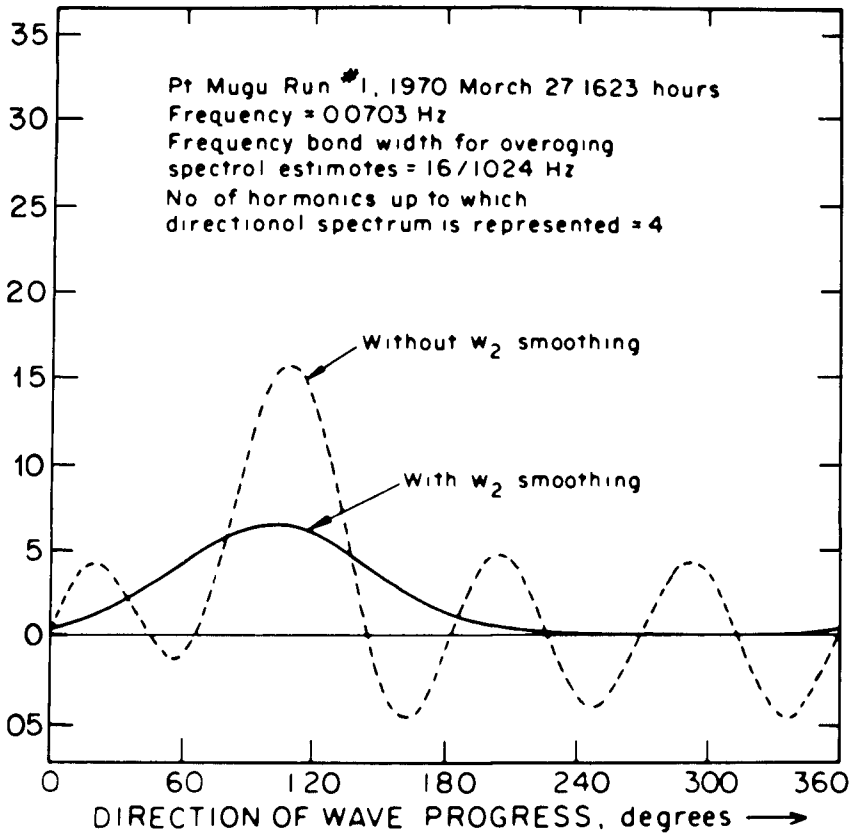

FIG. 3. DIRECTIONAL SPECTRUM OBTAINED FOR FREQUENCY 0.0703 Hz WITH AND WITHOUT W_2 SMOOTHING

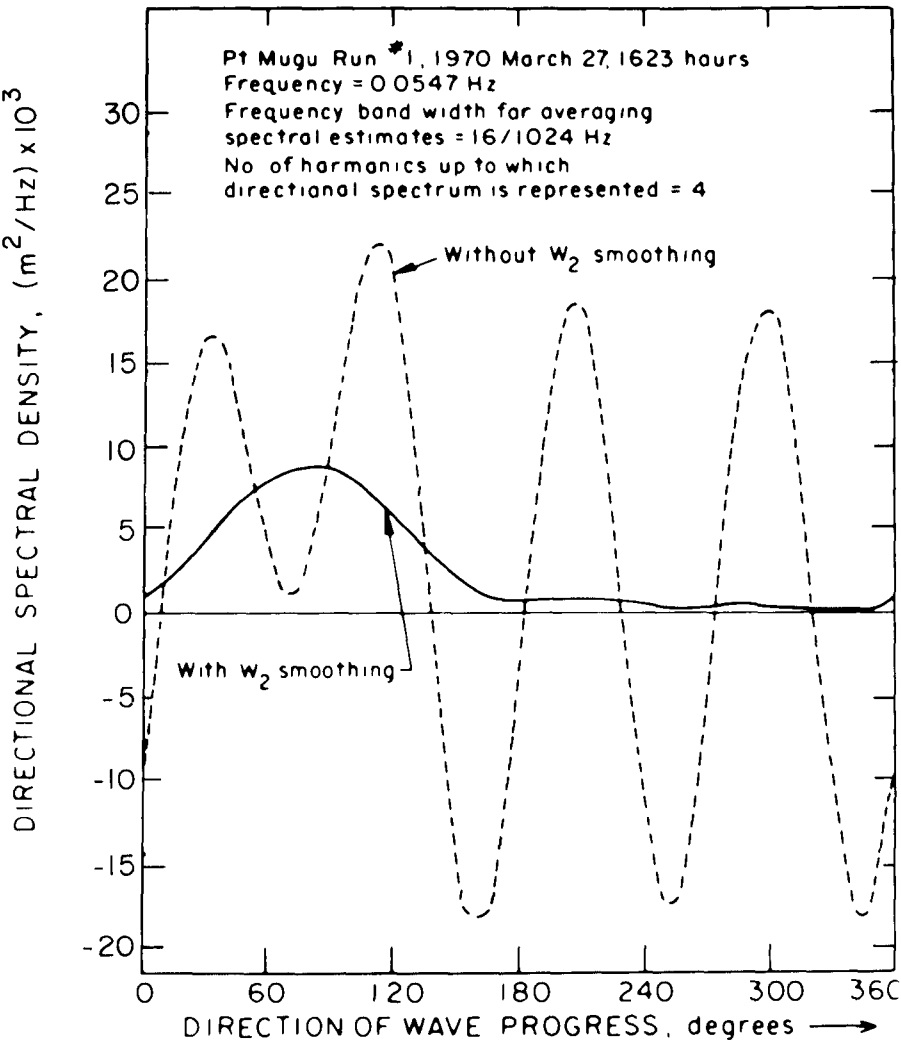

FIG. 4 DIRECTIONAL SPECTRUM OBTAINED FOR FREQUENCY 0.0547 Hz WITH AND WITHOUT W_2 SMOOTHING